DAΦNE TECHNICAL NOTE

INFN - LNF, Accelerator Division

Frascati, March 6, 1996

Note: **MM-11**

FIELD QUALITY OF THE SMALL SEXTUPOLES FOR THE DAΦNE MAIN RINGS

B. Bolli, F. Iungo, F. Losciale, N. Ganlin,
M. Preger, C. Sanelli, F. Sardone

1. Introduction

The 14 small sextupoles for the DAΦNE Main Rings, built by TESLA Eng. (U.K.), delivered to LNF together with the 60 small quadrupoles [1], have been measured with the rotating coil system [2] in order to check that each magnet meets the Specifications [3]. The results reported in this Note can be compared to those given in [3], where the measurements on the sextupoles for the DAΦNE Accumulator, of the same type of those described here, are presented.

The measurements have been performed at four excitation currents (≈ 100, 200, 280 and 340 A): the corresponding gradients (second derivatives of the field at the magnet centre) are ≈ 64, 128, 179 and 213 T/m^2 respectively. The magnetic length is 105 mm [3]. The maximum gradient required in the nominal Main Rings lattices is ≈ 80 T/m^2: much larger gradients are available, since we have chosen the same sextupoles as the Accumulator ones, where higher gradients are required. Of course, this enhances the overall flexibility of the Main Rings magnetic structure.

The position of the magnetic centre has also been recorded with respect to the reference optical devices placed on top of the magnets. The mechanical centre positions, however, have not yet been measured for lack of time, and therefore the distance between magnetic and mechanical centres is not yet available. This important part of the magnet characterisation, which takes into account the tilt of the magnet axis (not detectable by the rotating coil system) will be performed as soon as possible by the Alignment Group.

2. Integrated gradient

Table I gives the integrated gradients measured for each sextupole at the above mentioned excitation currents. Figure 1 is an histogram of the same result at 200 A. It is clear that the first two magnets (Serial#1 and Serial#2) are stronger than the others by ≈0.7% at all currents. This deviation could not been explained by a difference in steel length or bore diameter. However, it is not harmful for the operation of the ring, because each magnet has its own independent power supply.

Figure 2 gives the average value of the integrated gradient versus the excitation current (linear over the whole measured range), while Figure 3 plots the r.m.s. width of the distributions taking into account all sextupoles, or excluding the first two magnets.

Table I - Integrated gradients (second derivative, T/m)

Serial #	**100.51 A**	**200.91 A**	**281.29 A**	**337.46 A**
1	6.73540	13.44170	18.77648	22.40675
2	6.74282	13.45570	18.78390	22.42452
3	6.70412	13.37903	18.68620	22.30272
4	6.69589	13.36295	18.66159	22.27427
5	6.69814	13.36661	18.66909	22.27901
6	6.69441	13.36254	18.65870	22.26910
7	6.69429	13.36010	18.65474	22.26208
8	6.68776	13.34832	18.64212	22.24627
9	6.69761	13.36548	18.66232	22.27465
10	6.69648	13.36314	18.66197	22.27199
11	6.69221	13.35378	18.65378	22.26463
12	6.68539	13.34283	18.63152	22.23866
13	6.68789	13.34968	18.64729	22.25058
14	6.68480	13.34215	18.62951	22.23546

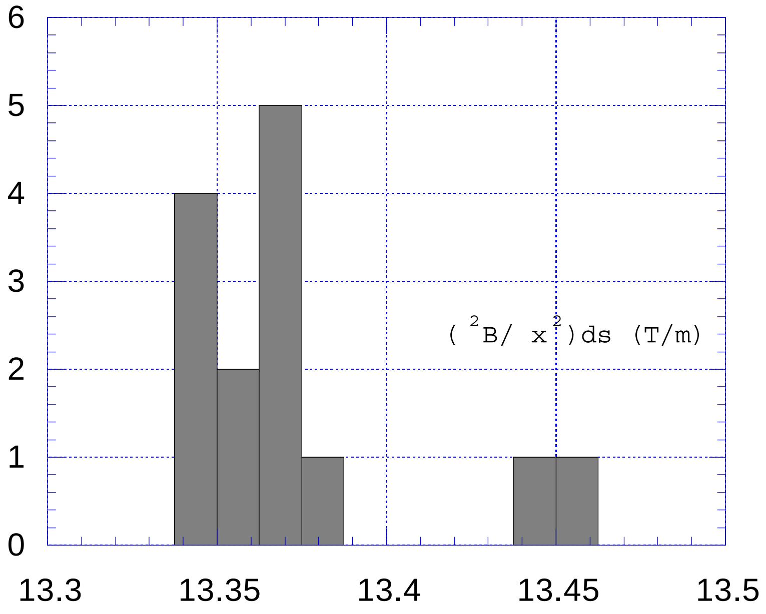

Figure 1. Distribution of integrated gradients among the 14 sextupoles.

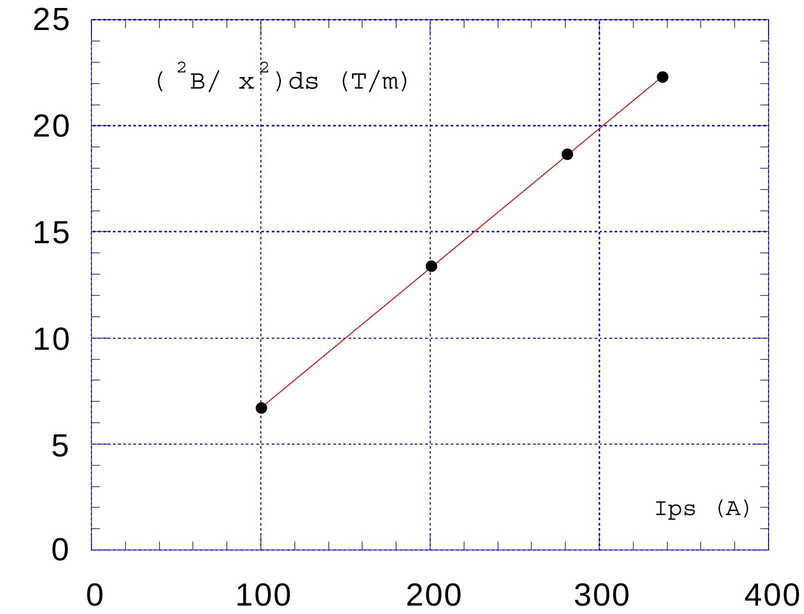

Figure 2. Integrated gradient versus current.

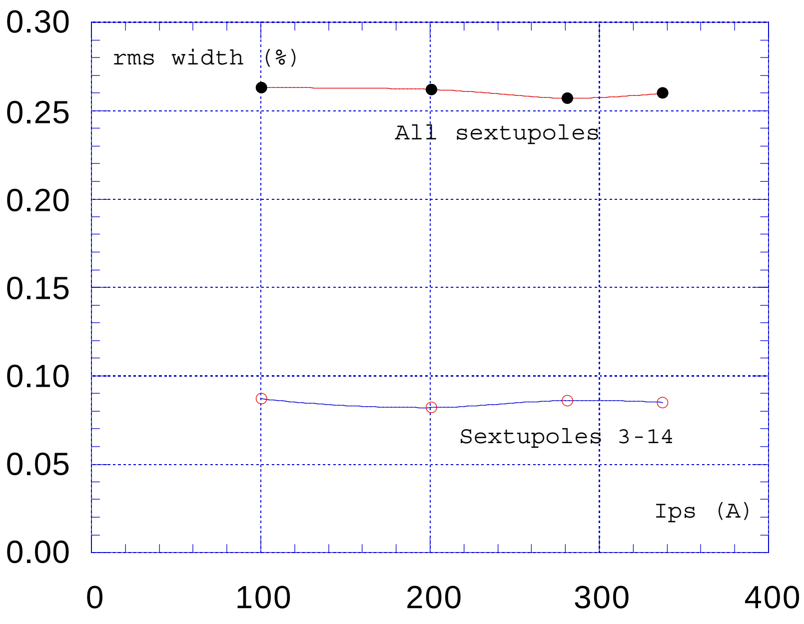

Figure 3. r.m.s. width of the integrated gradient distribution.

2. Average deviation from the ideal field

The average deviation of the field from the ideal sextupole (see [1] for the definition) at the boundary of the good field region is given in Table II for each sextupole.

Figure 4 is a typical output of the field deviation on the 30 mm radius circumference delimiting the good field region.

Figure 5 shows the average values versus the excitation current on an expanded scale. The error bars are the rms width of the distributions. The field quality is remarkably constant over the sample of magnets, with a very small deviation from the average. Significant contributions (larger than 10^{-4} with respect to the main sextupole component at 30 mm from the axis) come from octupole, decapole and 18-pole high order harmonics.

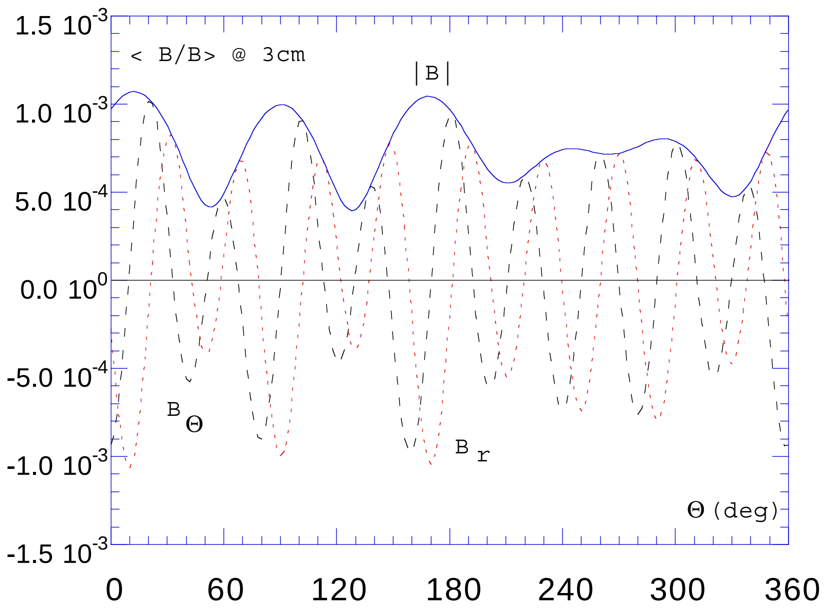

Figure 4. Field quality of Sextupole Serial#10 @ 200.91 A.

Table II - Average deviation from the ideal field at 30 mm from the magnet axis (units of 10^{-4})

Serial #	100.51 A	200.91 A	281.29 A	337.46 A
1	7.62	7.50	7.52	7.55
2	7.62	7.64	7.55	7.63
3	7.45	7.48	7.55	7.49
4	7.39	7.35	7.38	7.40
5	7.54	7.70	7.62	7.64
6	7.29	7.29	7.33	7.34
7	7.28	7.25	7.40	7.31
8	7.41	7.33	7.33	7.30
9	7.60	7.31	7.34	7.35
10	7.44	7.46	7.37	7.51
11	7.41	7.44	7.40	7.46
12	7.97	7.73	7.55	7.56
13	7.45	7.46	7.41	7.42
14	7.37	7.36	7.48	7.62

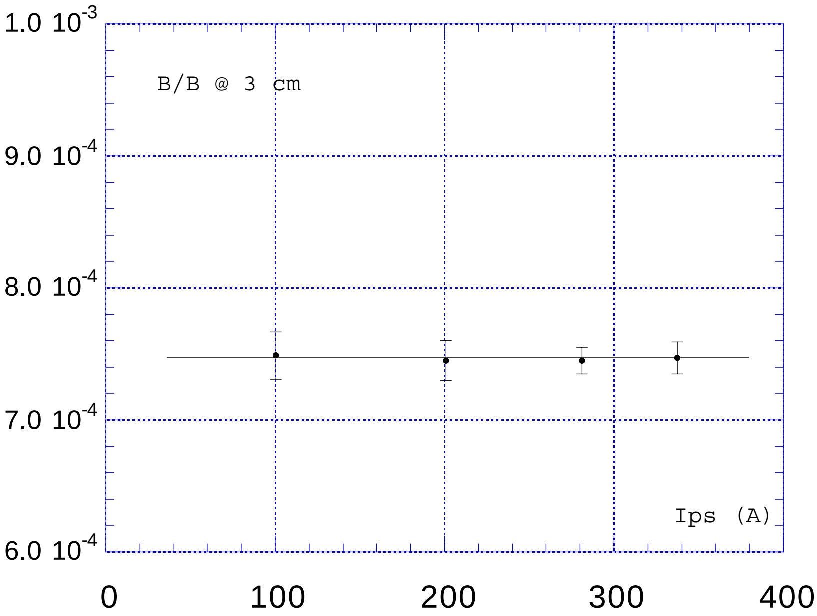

Figure 5 - Average deviation @ 30 mm averaged over the 14 magnets. Error bars are the r.m.s. widths of the distributions (expanded scale).

3. Octupole contribution

Table III lists the octupole component, divided by the main sextupole one for each magnet. Figure 6 shows an histogram of the distribution at 200.9 A.

Table III - Octupole/Sextupole @ 3 cm (units of 10^{-4})

Serial #	**100.51 A**	**200.91 A**	**281.29 A**	**337.46 A**
1	2.14	1.35	1.19	1.32
2	0.38	1.67	0.53	1.19
3	0.47	0.96	1.03	0.29
4	1.18	0.59	0.68	1.01
5	0.90	2.46	2.09	1.61
6	0.28	0.40	0.65	0.83
7	0.41	0.67	1.79	1.07
8	1.12	0.71	0.25	0.26
9	2.44	0.80	0.57	0.48
10	1.71	1.77	1.04	1.49
11	0.88	1.54	0.66	1.50
12	3.37	3.05	1.58	1.47
13	0.98	1.35	0.29	0.89
14	1.75	1.60	2.35	2.86

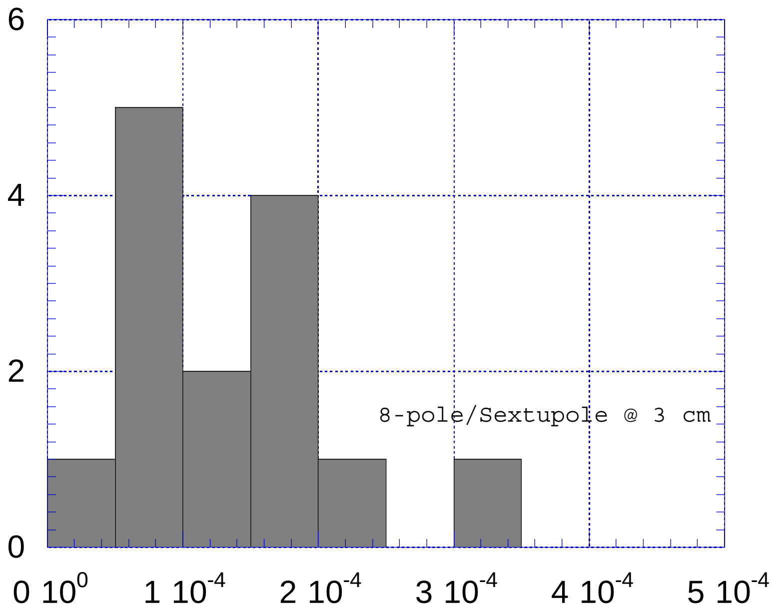

Figure 6. Octupole/Sextupole distribution @ 200.91 A.

Figure 7 gives the average values of the fractional octupole contribution with the r.m.s. widths of the distribution at the different excitation currents. Within these widths, the octupole term does not depend on the current and has a rather large random part. The phase is distributed at random.

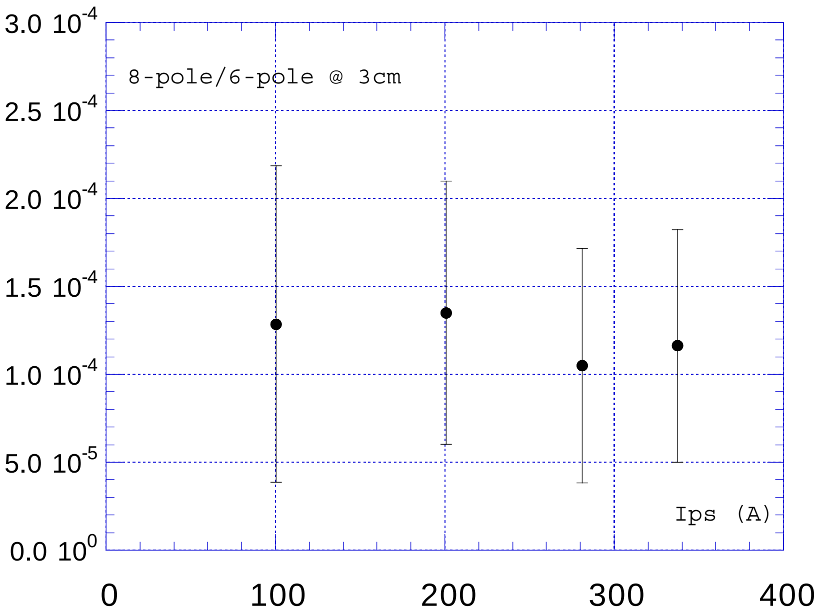

Figure 7 - Octupole/Sextupole @ 30 mm averaged over the 14 magnets. Error bars are the r.m.s. widths of the distributions.

4. Decapole contribution

The ratio between the decapole term and the sextupole one at the boundary of the good field region is given in Table IV, while Figure 8 is an example of the distribution of the sextupoles at 200.91 A. Figure 9 gives the average values and the r.m.s. widths of the distributions versus the excitation current: in this case the random part is smaller than in the case of the octupole. The phase is opposite to the main sextupole one, with a fluctuation of ≈±10 degrees.

Table IV -Decapole/Sextupole @ 3 cm (units of 10^{-4})

Serial #	100.51 A	200.91 A	281.29 A	337.46 A
1	1.93	1.71	1.77	1.67
2	2.21	1.92	1.84	1.78
3	2.27	2.24	2.45	2.35
4	1.58	1.59	1.46	1.73
5	2.64	2.55	2.60	2.63
6	1.62	1.66	1.49	1.29
7	1.26	1.21	1.51	1.27
8	1.70	1.42	1.43	1.16
9	1.99	1.83	1.88	1.63
10	2.00	1.81	1.91	2.03
11	1.85	1.77	1.82	1.71
12	2.70	2.34	2.37	2.57
13	2.09	1.81	1.93	1.69
14	1.17	1.22	1.20	1.43

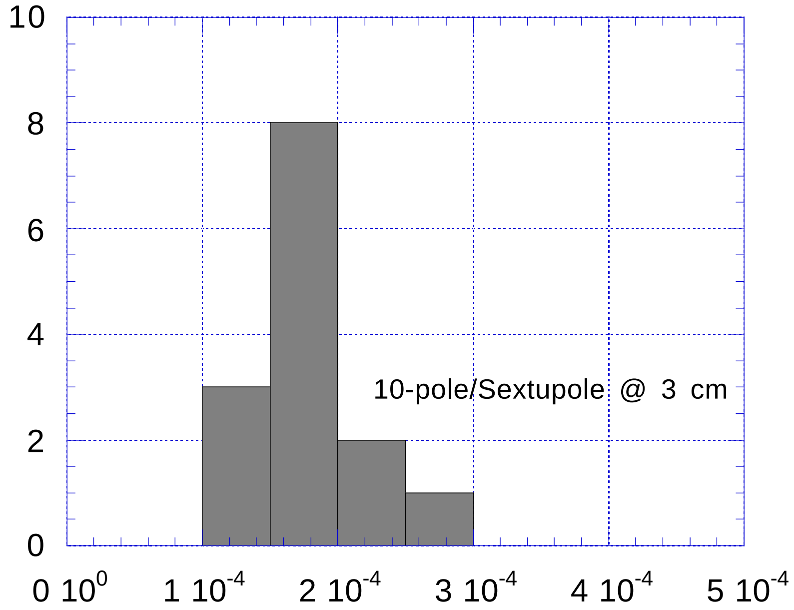

Figure 8. Decapole/Sextupole distribution @ 200.91 A.

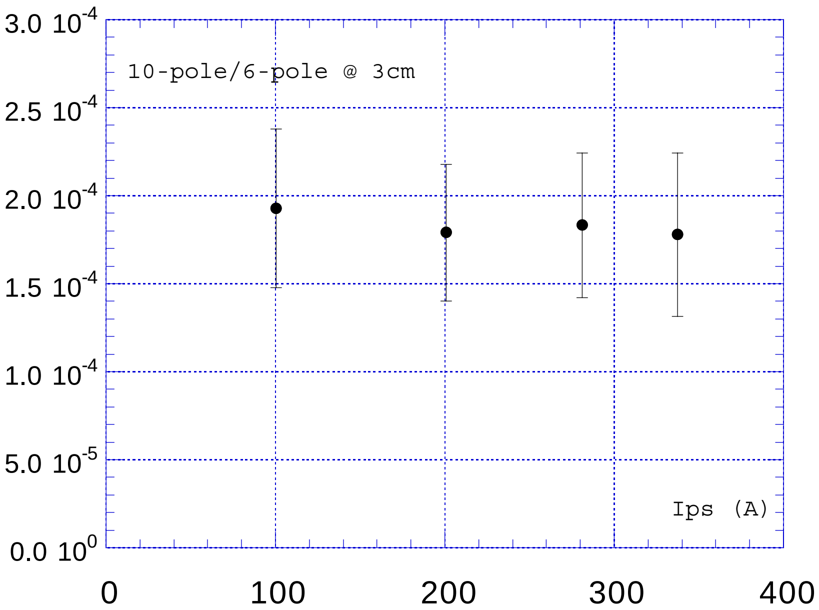

Figure 9 - Decapole/Sextupole @ 30 mm averaged over the 14 magnets. Error bars are the r.m.s. widths of the distributions.

5. 18-pole contribution

The 18-pole, as expected, is the largest contribution to the overall deviation from the ideal field. Table V gives its fractional contribution at the boundary of the good field region. Figure 10 is an example of the distribution at 200.91 A.

Table V - 18-pole/Sextupole @ 3 cm (units of 10^{-4})

Serial #	100.51 A	200.91 A	281.29 A	337.46 A
1	7.31	7.32	7.35	7.39
2	7.43	7.38	7.41	7.45
3	7.24	7.25	7.28	7.28
4	7.24	7.24	7.28	7.24
5	7.22	7.23	7.20	7.28
6	7.18	7.18	7.22	7.24
7	7.20	7.17	7.20	7.19
8	7.26	7.22	7.24	7.24
9	7.19	7.15	7.19	7.23
10	7.17	7.21	7.18	7.26
11	7.24	7.23	7.26	7.28
12	7.25	7.14	7.24	7.23
13	7.25	7.25	7.26	7.28
14	7.19	7.20	7.21	7.24

As the 18-pole is a systematic multipole with the same symmetry of the main sextupole component, the contribution of the 18-pole depends on the pole profile [3], and the distribution has a very small width around the average value. Figure 11 shows, on an expanded scale, the average value of the fractional contribution at 30 mm from the magnet axis. Error bars are the r.m.s. widths. The phase is always opposite to the main sextupole component.

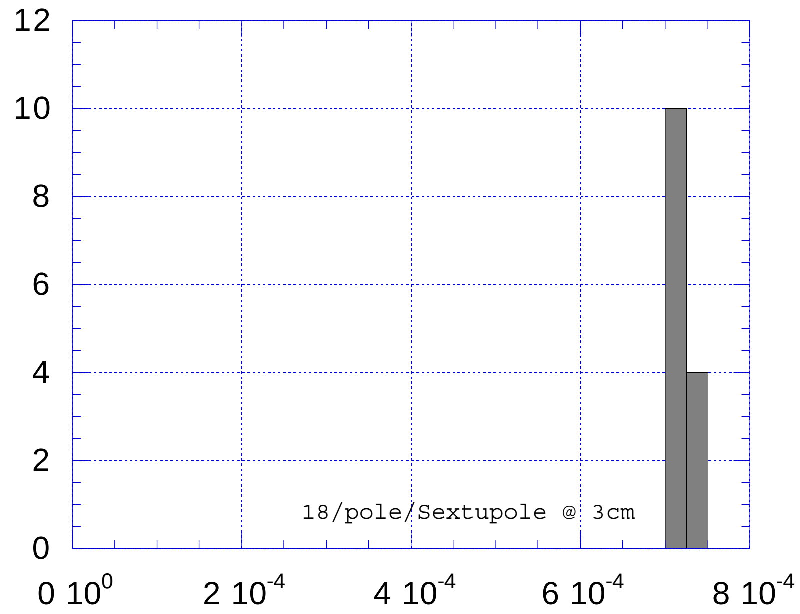

Figure 10. 18-pole/Sextupole distribution @ 200.91 A.

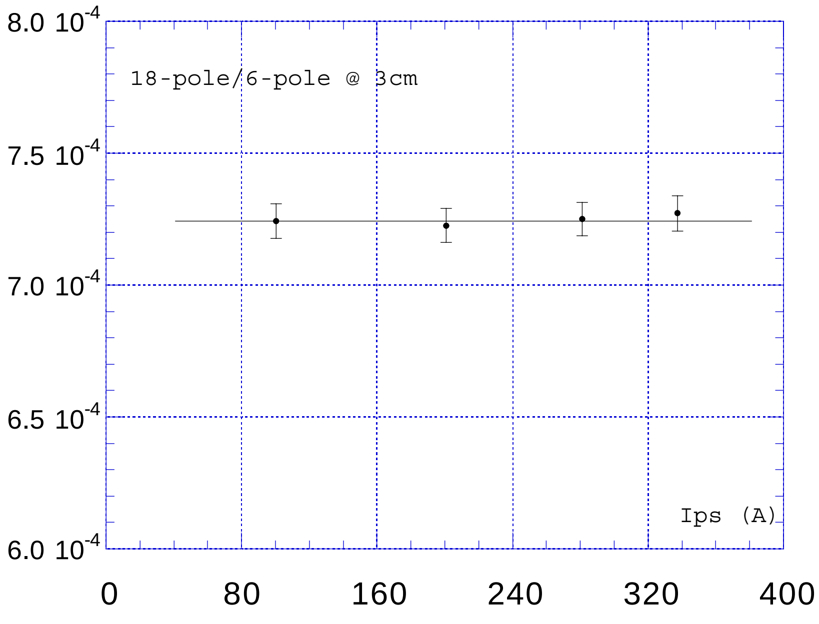

Figure 11 - 18-pole/Sextupole @ 30 mm averaged over the 14 magnets. Error bars are the r.m.s. widths of the distributions (expanded scale).

6. Conclusions

The results given in this note are consistent with those presented in [3] for the DAΦNE Accumulator sextupoles. There are no major differences between the magnets in the first batch of 8 magnets, built for the Accumulator, and the second one. Table VI is a summary of systematic and random errors for the small sextupoles, to be used in lattice simulations with errors.

Table VI - Systematic and random multipoles
(expressed as fraction of main sextupole field at 30 mm, units of 10^{-4})

Multipole	Systematic	Phase (deg)	Random (rms)	Phase (deg)
8-pole	1.21	random	0.74	random
10-pole	1.83	180	0.43	180
18-pole	7.25	180	0.06	180

References

[1] B. Bolli, F. Iungo, F. Losciale, N. Ganlin, M. Preger, C. Sanelli, F. Sardone "Field quality of the small quadrupoles for the DAΦNE Main Rings" - DAΦNE Technical Note MM-10 (22/2/96).

[2] F. Iungo, M. Modena, Q. Qiao, C. Sanelli "DAΦNE magnetic measurement systems" - DAΦNE Technical Note MM-1 (2/12/94).

[3] B. Bolli, F. Iungo, M. Modena, M. Paris, M. Preger, C. Sanelli, F. Sardone, F. Sgamma, M. Troiani "The DAΦNE Accumulator sextupoles" - DAΦNE Technical Note MM-6 (10/5/95).